Carbon Deposition and Deuterium Inventory in ASDEX Upgrade

M. Mayer[1], V. Rohde[1], J. Likonen[2], E. Vainonen-Ahlgren[2], J. Chen[1], X. Gong[1], K. Krieger[1], ASDEX Upgrade Team

[1] Max-Planck-Institut für Plasmaphysik, EURATOM Association, Boltzmannstr. 2, D-85748 Garching, Germany
[2] VTT Processes, Association EURATOM/TEKES, P.O. Box 1608, FIN-02044 VTT, Finland
e-mail: Matej.Mayer@ipp.mpg.de

Abstract Carbon erosion and deposition in the ASDEX Upgrade divertor was investigated using a poloidal section of marked divertor tiles and silicon samples below the divertor structure. The whole inner divertor is a net carbon deposition area, while a large fraction of the outer divertor is erosion dominated and the roof baffle tiles show a complicated distribution of erosion and deposition areas. In total, 43.7 g B+C were redeposited, of which 88% were deposited on tiles and 9% in remote areas (below roof baffle, on vessel wall structures). Identified carbon sources in the main chamber are too low by a factor of ten to explain the observed carbon divertor deposition, but carbon erosion is observed at the outer divertor tiles. Deuterium is trapped mainly on the surfaces of the inner divertor tiles. The long term retention in codeposited hydrocarbon layers is about 3% of the total deuterium fuel input.

1. Introduction

Major disadvantages of carbon as plasma facing material are its high chemical erosion yield by hydrogen bombardment [1], and its ability to trap large amounts of hydrogen by codeposition [2]. It has been shown previously at JET and ASDEX Upgrade, that carbon is eroded in the main chamber and redeposited preferentially in the inner divertor [3–7]. Increasing coverage of the ASDEX Upgrade walls with tungsten allows a more detailed identification of remaining carbon erosion areas. Carbon limiters at the low field side were identified as carbon sources [5], while the tungsten coated inner heat shield serves as carbon recycling area [5]. Carbon deposition on some ASDEX Upgrade divertor tiles was studied by secondary ion mass spectrometry (SIMS), resulting in a deposition of about 15×10^{19} C-atoms/s [4]. This is about five times larger than the observed main chamber carbon source. Although these numbers are based on only few data points and are subject to large errors, they indicate either the existence of additional carbon sources, or much larger experimental errors than assumed by the experimentalists.
Data about net carbon erosion are scarce due to the experimental difficulties of erosion measurements. Carbon erosion/deposition was studied in some detail at the TEXTOR limiter [8], and there is some indication about net carbon erosion in the outer divertors of JET and DIII-D [7,9]. This paper presents data about integrated carbon erosion/deposition in the ASDEX Upgrade divertor, measured post mortem with quantitative ion beam analysis methods and SIMS.

2. Experimental

The ASDEX Upgrade divertor IIb is shown in Fig. 1. Tiles 6A and 6B form the inner baffle, tiles 9A, 9B and 9C the roof baffle, and tiles 2 and 3 the outer baffle. Tile 4 is the inner strike point tile, and tiles 1_{low} and 1_{up} the outer strike point tiles. Most tiles consist of fine grain graphite, while tile 4 is made from carbon-fibre composite (CFC). All tiles 6A and 6B were coated with W in summer 2002, except the two tiles used for this analysis.
A poloidal section of tiles was coated with a marker consisting of 1.6×10^{18} Re-atoms/cm^2 (about 230 nm), and 3.1×10^{19} (about 3.1 μm[1]) carbon on top using a pulsed plasma arc. The outer strike point tiles 1_{low} and 1_{up} were covered with a thicker carbon layer of 7.5×10^{19} (about 7.5 μm). The Re serves as marker for ion beam analysis and SIMS, allowing to measure the thickness of the overlaying carbon layer.

[1] For simplicity we use a carbon density of 1×10^{23} at/cm^3 = 2 g/cm^3 throughout this paper.

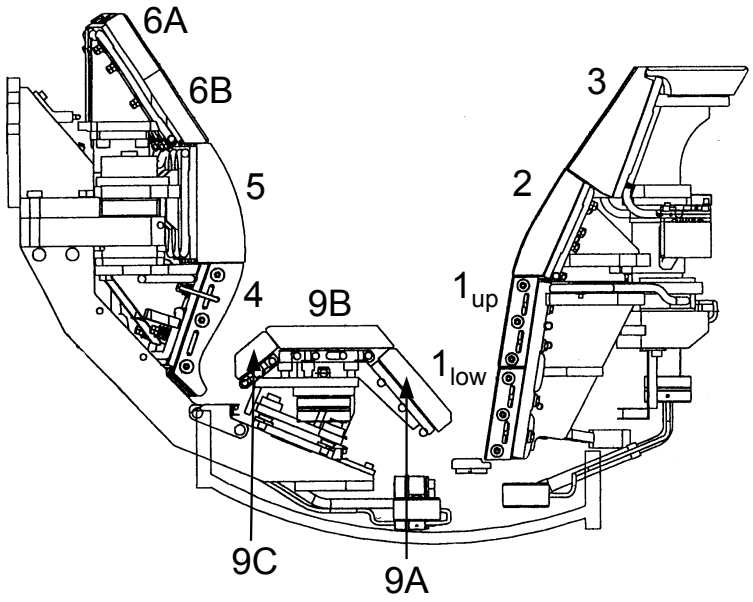

Figure 1: ASDEX Upgrade divertor IIb. Numbers indicate tile numbers.

The tiles were analyzed prior to installation with Rutherford-backscattering (RBS) using 1.6 MeV protons at 165°. The tiles were analyzed again after exposure using RBS under the same conditions. For thicker layers 2.5 MeV protons were used. The information depth at this energy is about 26 μm. Deuterium was detected using nuclear reaction analysis (NRA) using 0.8 and 2.5 MeV ^{3}He, having information depths of 1.3 and 8 μm^2. The spectra were evaluated with the program SIMNRA [10–12].
Secondary ion mass spectrometry (SIMS) measurements were performed using a scanned beam of 5 keV O_2^+ [13]. The depth calibration was obtained by measuring the SIMS crater depth with a profiler.
The tiles were installed in 11/2002 and replaced in 08/2003. 1237 plasma discharges with 4944 s plasma in divertor configuration were performed during the discharge period. Six boronizations and one siliconization were applied during this time for wall conditioning. The siliconization was performed 2 weeks (about 150 discharges) before the end of the discharge period.

3. Results and discussion

3.1. Strike point position The distribution of strike point positions during the discharge period is shown in Fig. 2 (top). The s-coordinate is measured along the tile surfaces. The inner strike point was mostly on tile 4, the outer strike point was on tiles 1_{low} and 1_{up}. Some discharges had their strike point on roof baffle tile 9B.

3.2. Carbon erosion and deposition Net deposition and erosion of boron + carbon on the tiles is shown in Fig. 2 (bottom). The sum of B + C can be determined accurately with RBS from the energy shift of the Re peak, but the discrimination of both elements is difficult due to overlap of the sub-spectra. The B/C ratio in redeposited layers could be determined only close to the surface of sufficiently thick layers, where it was in the range 0.1–0.2. Boron originates from regular boronizations for wall conditioning [14], during which about 60 nm of amorphous hydrogen-boron layer are deposited on the main chamber walls. Only small amounts are deposited in the divertor due to the closed geometry. From the walls it is subsequently eroded

[2]These depths are for pure carbon. The information depths are larger by about 50% in deuterium-rich hydrocarbon layers with D/C $\approx$ 1.

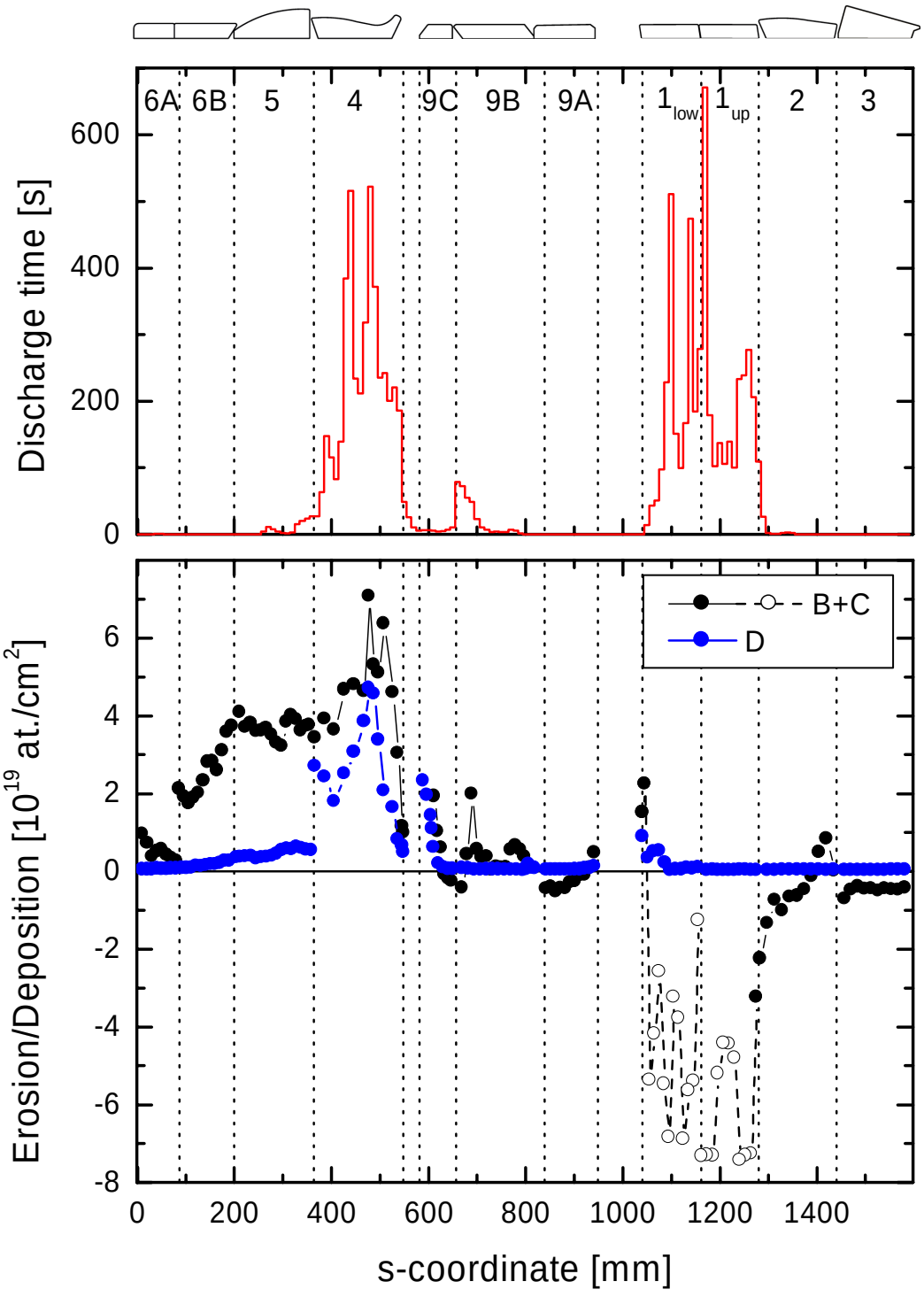

Figure 2: Top: Distribution of strike point positions (from magnetic reconstruction) during the discharge period 2002/2003 together with a schematic representation of the tiles. Histogram width 10 mm. Bottom: Black solid and hollow dots: Erosion of carbon and deposition of boron + carbon on the divertor tiles. Positive numbers indicate deposition, negative numbers erosion. The data on tiles 1_{low} and 1_{up} (hollow dots) are subject to large errors due to complete loss of the marker layer and should be interpreted with care. Blue dots: Deuterium inventory.

and redeposited in the divertor. Small amounts of silicon are visible at the surface due to the siliconization, and oxygen is present at a level of 5–15 at%. Other elements like Fe and W are detected only in small quantities [15].
The whole inner divertor is a net carbon deposition area. The thickest deposits are observed on the inner strike point tile 4, but tile 5 and a fraction of tile 6B show also thick deposits, although the strike point was never on these tiles. Tile 6A shows only smaller deposits.
A complicated distribution of net deposition and erosion areas is observed on the roof baffle. Tile 9C shows deposition at the surface facing the inner strike point. Deposition is also observed on tile 9B in the region of the roof baffle strike point position. Some erosion is observed on tile 9A, followed by small deposition just opposite the outer strike point. In total, the effects on the roof baffle tiles are small, compared to the inner and outer divertor.
The outer baffle (tiles 2 and 3) is a net carbon erosion area, and the erosion ranges from 0.5–2.5 μm. Deposition is observed in areas shadowed by neighboring tiles, like the area on tile 2 close to tile 3 ($s = 1400 - 1440$ mm). Boron and carbon deposition is also observed on a small fraction of the bottom part of tile 1_{low} ($s = 1040 - 1050$ mm), where the strike point was never positioned. The outer strike point area on tiles 1_{low} and 1_{up} shows strong erosion, and the whole initial carbon and a large fraction ($> 90\%$) of the Re marker layer have disappeared on most of the tile surface, i.e. the erosion exceeds 7.5 μm carbon. The Re marker was still present in the deposition area on the bottom part of tile 1_{low}, and on a small fraction of tile 1_{up} close to tile 2 ($s = 1280$ mm): In this area the initial carbon layer thickness decreased from 6.8 to 3.7 μm.
Due to the total disappearance of the C-layer and the Re marker the interpretation of tiles 1 is difficult, because it cannot be excluded that the observed erosion is due to mechanical failure of the marker layer instead of sputtering [16]. Therefore the results on the outer strike point tiles 1 should be treated with care.
Total amounts of redeposited B+C and eroded C, assuming toroidal symmetry, are summarized in Table 1. Carbon is mainly redeposited in the inner divertor and on roof baffle tile 9C. This is a striking difference to the deposition of tungsten: Tungsten is eroded in the main chamber, and deposited in similar fractions both in the inner and the outer divertor [15]. Carbon deposition is also observed below the roof baffle and other remote wall areas, but these amounts are small compared to the deposition on the inner divertor tiles. Deposition is also observed in some areas of the outer divertor, but this is more than counterbalanced by erosion at the outer baffle and outer strike point, resulting in net erosion in the outer divertor. Due to total erosion of the carbon marker layer only a lower bound for the erosion can be given.
Erosion from the main chamber outboard limiters was determined spectroscopically during the 2001/2002 campaign and extrapolated to the 2002/2003 campaign investigated in this work. Additionally, there is is a total flux of 11.5 g carbon originating from the inner heat shield [5]. However, as the inner heat shield is coated with tungsten, this carbon influx is not a primary carbon source, but has been interpreted as carbon recycling [3,4].
The amounts of eroded and redeposited carbon in Table 1 suggest, that the outer divertor is the major carbon source. Carbon is then subsequently transported to the inner divertor, where it is redeposited. Carbon limiters in the main chamber act as additional carbon sources, but their source strength is lower by a factor of ten compared to the outer divertor. However, this interpretation should be taken with some care, because, as already pointed out, the marker layers could have been lost due to mechanical failure (delamination) instead of erosion [16].
Despite these uncertainties, it can be concluded that carbon erosion occurs in the outer divertor. This erosion is at least equivalent, if not exceeding, carbon erosion in the main chamber. Additional measurements, which might clarify the puzzle, are foreseen for the discharge period 2004/2005.

	Erosion	Deposition	
	C	B+C	D
	[g]	[g]	[g]
Inner divertor	0	27.3	1.5
Roof baffle	-0.6	2.9	0.18
Outer divertor	$<$ -38.3	9.5	0.14
Behind inner heat shield [17]	0	0.4	0.07
Below roof baffle + vessel [17]	0	3.6	0.49
Pumped out[4]	0	0.6	n.a.
Outboard main chamber limiter[5]	-2.6	?	?
Total	$<$ **-41.5**	**44.3**	**2.4**

Table 1: Carbon erosion/deposition and deuterium inventory for the discharge period 2002/2003. Inner divertor summarizes erosion/deposition on tiles 4–6B, roof baffle summarizes tiles 9A–9C, and outer divertor summarizes tiles 1_{low} to 3. Below roof baffle + vessel summarizes the areas below the roof baffle, the vessel area below the roof baffle, pump ducts, and the LN_2-shield of the cryogenic pump. Deuterium is mainly pumped out as D_2, which is not accounted here.

3.3. Deuterium inventory The deuterium inventory on the tile surfaces is shown in Fig. 2. D is mainly trapped in codeposited, deuterium-rich hydrocarbon layers on the inner strike point tile 4 and on tile 9C just opposite the inner strike point. The D/C ratio of these layers is in the range 0.5–0.9. Some D is also trapped in layers deposited on tiles 5 and 6B. SIMS measurements and NRA at different energies show, that the D is inhomogeneously distributed in the layers on these tiles: It is concentrated in the near-surface region of the layer, while the deuterium concentration is smaller deeper inside the layers. This is an indication that the layers lost a large fraction of their trapped deuterium inventory after about 2/3 of the discharge period, probably due to elevated surface temperatures.
The outer strike point tiles show only small amounts of trapped D ($< 3 \times 10^{18}$ D/cm^2) due to high surface temperatures, especially during high power discharges. The only exception is the lowest part of tile 1_{low}, where about 2 μm thick, deuterium-rich layers with a D/C ratio of about 0.6 are observed. These layers are only observed in areas, where the strike point was never positioned. Tiles 2 and 3 are erosion dominated and show only small deuterium inventories.
Deuterium-rich layers with D/C from 0.4–1 are observed on the structure and wall below the divertor roof baffle [18,17,19]. The deuterium concentration in the layers depends on the flux of high-energetic particles and temperature: The highest deuterium concentrations (with D/C $\approx$ 1.7) are observed on the liquid-nitrogen cooled heat shield of the divertor cryo-pump. The thickest layers are observed close to the strike points, and layers in the inner divertor are about 3 times thicker than in the outer divertor.
The deuterium inventories on the divertor tiles, of all areas below the roof baffle, the vessel area below the roof baffle, pump ducts, and the LN_2-shield of the cryogenic pump, are summarized in Table 1. In total, 2.4 g deuterium were trapped inside the vessel, of which the majority (about 75%) are trapped on the tiles of the inner divertor. The inventory trapped in remote areas (below roof baffle etc.) is smaller by a factor of three compared to the inventory on the tiles.
The total deuterium input into plasma discharges by gas puffs, neutral beam injection and pellets was about 75 g for the whole discharge period. Additionally about 2 g of D were introduced into the vessel as D trapped in boronized layers during boronizations, resulting in a total deuterium input of about 77 g for the whole discharge period. The observed deuterium trapping inside

the vessel is therefore only about 3% of the total deuterium input. This low value is in some disagreement with gas balance measurements [20], which gave a retention of 10–20% of the input. This discrepancy might be due to the large errors of gas balance measurements, or might be due to outgassing of large amounts of D from deposited layers on divertor tile surfaces during singular events, such as disruptions or high-power discharges, if the tile surfaces get hot. There is some indication that this happened with tiles 5 and 6B.

3.4. Mechanism of layer formation in remote areas As already mentioned above, the layer thickness distribution below the roof baffle is strongly inhomogeneous: The thickest layers are observed close to the strike points, and the layer thickness decreases about exponentially with increasing distance to the strike points [18,21]. This lateral variation shows qualitatively, that the layers are formed mainly by particles with high sticking probability to the walls [21,22,4]. This observation is confirmed by measurements of the surface-loss probability of hydrocarbon radicals with sticking monitors below the divertor structure, which gave a surface-loss probability of 0.65–0.75 [23]. Possible hydrocarbon radical species responsible for this deposition are C_2D, which has a surface-loss probability of 0.8 [24], or C_2D_3 with a surface-loss probability of 0.35 [24]. The amount of layer deposition in very remote areas (such as pump ducts) is small [18], indicating either a small contribution of hydrocarbon radicals with low sticking coefficient (such as CD_3, which has a sticking coefficient in the range 0.0001–0.01), or a re-erosion rate exceeding the sticking coefficient. A parasitic plasma is observed below the roof baffle [17,25,26], creating hydrogen atoms and ions. These particles can change the sticking coefficient, and can also re-erode already deposited layers. Time resolved measurements using quartz micro-balances below the roof baffle [17] showed a continuous layer growth in the inner divertor, while the layer growth rate in the outer divertor depends on the discharge scenario: In some cases even erosion rather than deposition is observed.

4. Conclusions

Carbon deposition and carbon erosion were measured on ASDEX Upgrade divertor tiles and below the divertor roof baffle. The inner divertor is a net carbon deposition area, while a large fraction of the outer divertor is erosion dominated and the roof baffle tiles show only minor effects. The B+C deposition on divertor tile surfaces is about 10 times larger than in remote areas like below the roof baffle, vessel wall structures and pump ducts. Identified carbon sources in the main chamber are carbon limiters at the outboard side. However, the observed carbon erosion from these limiters is lower by a factor of 10 compared to carbon deposition. Carbon erosion is observed in the outer divertor, indicating that the outer divertor is a net carbon source, which might exceed the carbon source in the main chamber by a factor of 10. However, as the applied marker technique might give incorrect results in the case of mechanical failure of the layers, the primary carbon sources in ASDEX Upgrade remain unclear and require additional measurements.

Deuterium is mainly trapped on the inner divertor tiles. The deuterium inventory in remote areas is smaller by a factor of three compared to the inventory on the tiles. Deuterium-rich layers below the divertor roof baffle are created by sticking of hydrocarbon radicals with high sticking probability to the walls. The long-term retention, as measured by surface analysis, is about 3% of the deuterium input.

Acknowledgements Ion beam analysis measurements by T. Utikal and the technical assistance of J. Dorner and M. Fußeder are gratefully acknowledged.

References

[1] BALDEN, M. et al., J. Nucl. Mater. **280** (2000) 39.
[2] MAYER, M. et al., J. Nucl. Mater. **290-293** (2001) 381.

[3] MAYER, M. et al., Physica Scripta **T111** (2004) 55.
[4] ROHDE, V. et al., Physica Scripta **T111** (2004) 49.
[5] PüTTERICH, T. et al., Plasma Phys. Controlled Fusion **45** (2003) 1873.
[6] COAD, J. et al., J. Nucl. Mater. **290-293** (2001) 224.
[7] COAD, J. et al., J. Nucl. Mater. **313-316** (2003) 419.
[8] MAYER, M. et al., J. Nucl. Mater. **313-316** (2003) 377.
[9] WHYTE, D. et al., Nucl. Fusion **39** (1999) 1025.
[10] MAYER, M., SIMNRA user's guide, Technical Report IPP 9/113, Max-Planck-Institut für Plasmaphysik, Garching, 1997.
[11] MAYER, M., SIMNRA, a simulation program for the analysis of NRA, RBS and ERDA, in *Proceedings of the 15th International Conference on the Application of Accelerators in Research and Industry*, edited by DUGGAN, J. L. et al., volume 475 of *AIP Conference Proceedings*, page 541, American Institute of Physics, 1999.
[12] MAYER, M., Nucl. Instr. Meth. **B194** (2002) 177.
[13] VAINONEN-AHLGREN, E. et al., J. Nucl. Mater. (2005), this conference.
[14] ROHDE, V. et al., Comparison of boronization and siliconization in ASDEX Upgrade, in *26th EPS Conference on Controlled Fusion and Plasma Physics*, volume 23J of *europhysics conference abstracts*, page 1513, 1999.
[15] K.KRIEGER et al., J. Nucl. Mater. (2005).
[16] MAYER, M. et al., J. Nucl. Mater. (2005), in print.
[17] ROHDE, V. et al., J. Nucl. Mater. (2005), in print.
[18] MAYER, M. et al., J. Nucl. Mater. **313-316** (2003) 429.
[19] ROHDE, V. et al., J. Nucl. Mater. **290-293** (2001) 317.
[20] MERTENS, V. et al., Hydrogen gas balance in ASDEX Upgrade with div IIb, in *30th EPS Conference on Controlled Fusion and Plasma Physics*, europhysics conference abstracts, 2003.
[21] MAYER, M. et al., Mechanism of hydrocarbon layer formation in remote areas of fusion devices, in *30th EPS Conference on Controlled Fusion and Plasma Physics*, volume 27A of *europhysics conference abstracts*, pages O–2.6A, 2003.
[22] ROHDE, V. et al., Physica Scripta **T103** (2003) 25.
[23] MAYER, M. et al., Temperature dependence of hydrocarbon layer growth in remote areas of fusion devices, To be published, 2005.
[24] HOPF, C. et al., J. Appl. Phys. **87** (2000) 2719.
[25] ROHDE, V. et al., J. Nucl. Mater. **313-316** (2003) 337.
[26] ROHDE, V. et al., On the influence of parasitic plasma below the divertor structure of ASDEX Upgrade on the formation of a-C:H layers, in *30th EPS Conference on Controlled Fusion and Plasma Physics*, volume 27A of *europhysics conference abstracts*, page P1.154, 2003.